

# Application of an AC-AC converter within calibration board integrated in a Smart Electrical Energy Meter

Zakariae JEBRONI<sup>(1)</sup>, Hajar CHADLI<sup>(2)</sup>, Belkasem TIDHAF<sup>(3)</sup>, Elhassane CHADLI<sup>(4)</sup>

<sup>(1),(3)</sup>Laboratory of Embedded Electronics Systems and Renewable Energy, National School of Applied Sciences

<sup>(2),(4)</sup>Laboratory of Electronics and Systems, Faculty of Sciences Oujda

University Mohammed Premier, Morocco

<sup>(1)</sup>zakariae.jebironi@gmail.com, <sup>(2)</sup>chad.hajar@gmail.com, <sup>(3)</sup>tidhaf@yahoo.com, <sup>(4)</sup>e\_chadli@yahoo.fr

**Abstract**—In our research work we presented a structure of a smart electrical energy meter that integrates a calibration board to automate this process. To calibrate the electrical meter on site we need a power source that provides a known and stable AC voltage, instead of using the line voltage that we can't predict its value at the time of calibration. For this reason, we have designed an AC-AC converter that respects some specifications as output voltage RMS value, output current RMS value and stability... The chosen structure is an indirect AC-AC converter (AC-DC-AC converter). The DC-AC converter is a voltage source inverter (VSI). To control the switches, we have used a digital control based on feedforward technique to eliminate the input variations. In this paper we detail the structure of the converter, the calculation method of the error and of the correction. Finally we present the results of simulation on MATLAB, in temporal and spectral forms. These results valid our design by the stabilization of the AC output voltage and the very low THD.

**Index Terms**—AC-AC converter, unipolar SPWM technique, smart meter, auto-calibration, digital control.

## I. INTRODUCTION

Power converters have become an important research field. Renewable energy sources, as well as new energy management strategies, have forced us to develop applications based on power converters in order to be able to properly control this energy and to be able to eliminate defects if they exist.

Among the converters we can quote the DC-DC converters which are generally used in energy conversion applications coming from solar panels, and which supply a DC load [1], their objective is either to increase the voltage, or to decrease it. We can also find DC-AC converters called inverters where their objective is to convert a DC voltage into an AC voltage. This kind of converters can be used in applications such as Adjustable Speed Drives (ASDs), Uninterruptible Power Supplies (UPSs) [2], [3] and the coupling of a photovoltaic station to the electrical network [4]. These mentioned applications are a few among that exists. We can find this type of converters in two popular forms: Voltage Source Inverters (VSI) [5], or Current Source Inverters (CSI). For the VSI, the DC source is the voltage and we are interested by the voltage waveform at the output, while for the CSI, the DC source is the current and we are interested by the current waveform at the output. We also find the AC-AC converters, which are dedicated to

the conversion of an AC signal in another identical form but by changing one or several characteristics of the signal (e.g. the amplitude). In this paper we are interested by one type of these converters; the AC-DC-AC type; i.e. we redress the input signal to create a DC voltage source, then we use a VSI to create a stable AC voltage in the output regardless of the input variation.

In fact, in our research work we design a Smart Electrical Energy Meter (SEEM) dedicated to measure the energy from single-phase line of low-voltage customers. During our study, we proposed a method of calibration on-site of the SEEM [6]. Using this method we can calibrate the meter or control its accuracy remotely. In the proposed design of the SEEM (Figure 1), we added a calibration board that contains an AC-AC converter powered by electrical grid voltage and a load that consumes a known current (Figure 2(a)). In this paper we present the performed study to realize the converter in order to comply with some specifications and the choice of components of the load. We also present the numerical method of switches control to regulate the output AC voltage. Finally, we present results of the simulations performed on MATLAB Simulink.

## II. INTEREST AND SPECIFICATIONS

### A. Converter interest

The first energy meters were electromechanical meters. Since then, researchers and engineers developed measurement

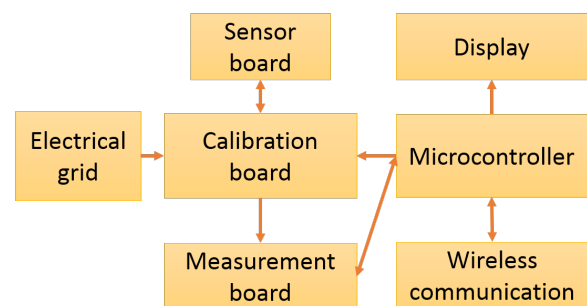


Fig. 1. Block diagram of the SEEM.

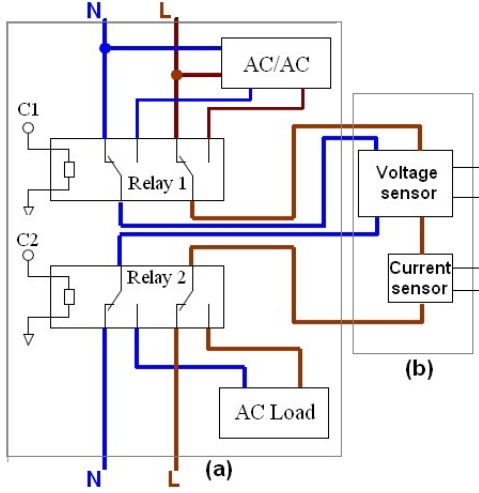


Fig. 2. Design of: (a) Calibration board; (b) Sensors board

instruments and added features that make some tasks easier.

Lately, the measurement instruments that have taken a very great importance were the Automatic Meter Reading (AMR). In these meters they added the notion of automatic recording of the energy consumed.

Currently, researchers are developing smart meters that can control and manage the electricity grid, i.e. balanced between the consumed and the produced energy. Moreover, using these meters, we can now easily couple several sources of energy to the electrical network and manage the whole. As we see, as researchers, we are trying to realize smart meters that are autonomous and totally remote controlled. Based on this hypothesis, we proposed a method to calibrate the SEEM on site and remotely. To perform this operation, it is necessary to integrate a power source which provides a known and fixed voltage and current. Indeed, when we want to perform a calibration of the meter we can not know what is the real value of the electrical grid voltage to take it as a reference. In Morocco, the electric operator guarantees a voltage variation between  $176V_{RMS}$  and  $253V_{RMS}$  for low voltage customers [7]. As a result, we included a calibration board within our system, controlled by the microcontroller. This board must contain a stable power source. So we designed an AC-AC converter powered by the electrical grid and provides a stable, known sinusoidal voltage at its output.

### B. Converter specifications

Referring to the article [6], we explained that we can use a single power point to calibrate the SEEM, we mentioned that this point preferably must correspond the maximum RMS voltage and the maximum RMS current. We also explained how we can use reference values below the maximum values. Therefore, before designing the AC-AC converter we have set these specifications:

- The converter must compensate the variations of the line voltage.

- The converter must provide a stable sinusoidal voltage equals  $120V_{RMS}$  at a line frequency and power a load that consumes  $5A_{RMS}$ .
- The load used must cause a  $60^\circ$  phase shift between the voltage and the current in order to compensate the phase shift that can be added by the system.
- The converter must contain the minimum of components while keeping a good result.

These points lead us to choose a structure of the converter presented in the following section. This converter, with H-bridge type, provides a power equals  $600VA$ , with a power factor equals  $0.5$ . To compensate for the variations of the input signal we used the feedforward technique, that is implemented numerically in a micro-controller. This micro-controller controls the switches by a PWM signal.

### III. AC-AC CONVERTER STRUCTURE

The system shown as block diagram in the figure 3 is an indirect, single-phase AC-AC converter. This system is supplied by the power grid. The electrical grid voltage in Morocco, for low voltage customers has a nominal RMS value equals  $220V$ . As mentioned, the voltage can vary between  $80\%$  and  $115\%$  of its nominal value. Therefore, we must prevent a compensation of this variation at time of the calibration.

The AC-AC converter contains several blocks. We will explain the operation of each of them, as well as the dimensioning and choice of components.

#### A. The rectifier

The AC/DC circuit shown in figure 4 is a full-wave single-phase rectifier, realized by means of a diode bridge and a Capacitor filter.

1) *Diode bridge*: Each diode in the off state must supports a peak reverse voltage equals (or superior) in absolute value to the maximum voltage of the electrical grid. The voltage line can reach  $253V_{RMS}$ , which corresponds to the maximum value  $357.8V$ . Therefore, for safety reasons, we choose diodes that support a peak reverse voltage equals  $400V$ .

The forward current of diodes is another important point for the choice of diode bridge. This current is the same DC link current supplying the inverter, and it is calculated by:

$$I_{DC} = \frac{V_o \cdot I_o}{V_{DC}} \cos \phi \quad (1)$$

Where  $V_o$  is the RMS value of the output voltage of the AC-AC converter,  $I_o$  is the RMS value of the output current

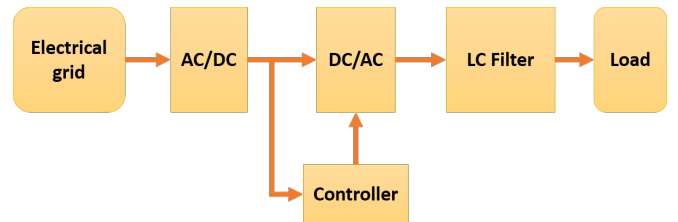


Fig. 3. Block diagram of the AC-AC converter.

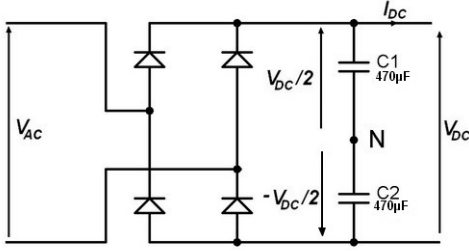


Fig. 4. Rectifier circuit.

of the AC-AC converter,  $\cos \phi$  is the power factor and  $V_{DC}$  is the DC voltage input of the inverter that provides from the rectifier.

We must calculate the maximum value of the DC current which circulates in diodes. A maximum current corresponds to a minimum DC voltage (according to the formula (1)). To determine the minimum DC voltage at the output of the rectifier, we have to consider the voltage ripple. The accepted direct voltage must be at least equal to the maximum voltage output of the converter, i.e. 170V. Of course, it is necessary to leave a safety marge and we choose a minimum voltage at the output of the rectifier equal to 200V. We calculate the maximum DC current for the values of different items of the formula (1). The value of the DC link current is:

$$I_{DC_{MAX}} = \frac{120 * 5}{200} * 0.5 = 1.5A$$

and we choose a value equal 2A.

2) *DC filter*: The most used filter in rectifiers is the capacitive one. We use filtering capacitors to reduce the voltage ripple and thus increase the value of the average input voltage. Formula (2) presents the relationship between the DC current, the voltage ripple, the value of the capacitor and the line frequency.

$$C = \frac{I_{DC}}{2.f.\Delta V_{DC}} \quad (2)$$

We will calculate the minimum value of the capacitor which corresponds to the maximum value of the voltage ripple and the minimum value of the DC current. As mentioned before, the minimum DC voltage accepted to supply the inverter is 200V and the line voltage decreases to 249V then the maximum ripple of the voltage is given by:

$$\Delta V_{DC_{MAX}} = 249 - 200 = 49V$$

The minimum DC current corresponds to the maximum value that can be reached by the electrical grid voltage. So the minimum DC current is:

$$I_{DC_{MIN}} = \frac{120 * 5}{358} * 0.5 = 0.84A$$

For these values of DC current and voltage ripple, we calculate the capacitor value:

$$C_{MIN} = \frac{0.84}{2 * 50 * 49} = 172\mu F$$

To create a neutral point N, as presented in figure 4 we used two capacitors in series and that they have the same value. These capacitors must support a voltage superior to  $V_{DC}/2$ . So, we choose capacitors with specifications 470 $\mu F$ , 200V

### B. The inverter

The inverter used in our converter is a VSI, H-bridge type. The inverter H-bridge shown in figure 5 contains four controlled switches and four feedback diodes. They exist another topologies most performed but that need more components, which is an inconvenient in our case. Furthermore, the simulation results show us that the use of this simple topology with a robust digital control is sufficient to reach our aim.

They exist several techniques to command the switches, and several researches [8]–[10] confirmed that the unipolar PWM technique gives a good results with a minimum THD.

In the unipolar PWM technique; called SPWM technique when we use sinusoidal modulating signal; we generate the PWM signal by comparing a carrier signal (generally triangular signal)  $V_c$  and two modulating sinusoidal signals  $V_r$  and  $-V_r$ . Figure 6 shows the waveform of carrier signal, modulating signals and pulses that control the switches. When  $V_r > V_c$  the switch  $S_1$  is on; similarly, when  $V_r < V_c$  the switch  $S_1$  is off. For the switch  $S_2$ , when  $-V_r > V_c$  the switch is on, and when  $-V_r < V_c$  the switch is off. Furthermore, the control of the switches  $S_4$  and  $S_3$  is the inverse compared to the switches  $S_1$  and  $S_2$  respectively. With this technique the inverter output can have three levels  $V_{DC}$ , 0 and  $-V_{DC}$ . Table I summarizes possible states that can take switches and the value of the inverter output  $V'_o$ . The output voltage of the inverter  $V'_o$  contains a fundamental component and harmonics. The fundamental component has the same frequency that the modulating signal, while the amplitude depends of the DC voltage and the amplitude modulation ratio  $m_a$  (also called modulation index) that is defined as:

$$m_a = \frac{V_{r_{MAX}}}{V_{c_{MAX}}} \quad (3)$$

Where  $V_{c_{MAX}}$  is the amplitude of the carrier signal and  $V_{r_{MAX}}$  is the amplitude of the modulating signal. In our application we work in the linear region of the modulation technique where  $m_a \leq 1$ . In this case, the fundamental amplitude corresponds to:

$$V'_{o1_{MAX}} = m_a V_{DC} \quad (4)$$

TABLE I  
SWITCHES STATES

State N	$S_1$ & $\bar{S}_4$	$S_2$ & $\bar{S}_3$	$V_{AN}$	$V_{BN}$	$V'_o$
1	ON	OFF	$V_{DC}/2$	$-V_{DC}/2$	$V_{DC}$
2	OFF	ON	$-V_{DC}/2$	$V_{DC}/2$	$-V_{DC}$
3	ON	ON	$V_{DC}/2$	$V_{DC}/2$	0
4	OFF	OFF	$-V_{DC}/2$	$-V_{DC}/2$	0

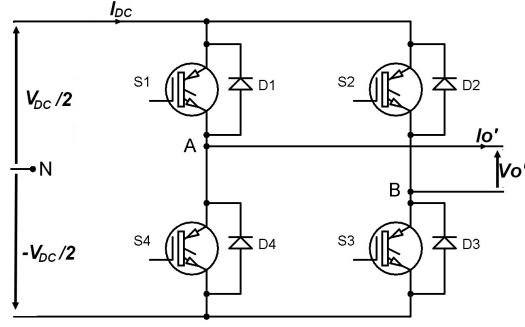


Fig. 5. Inverter circuit.

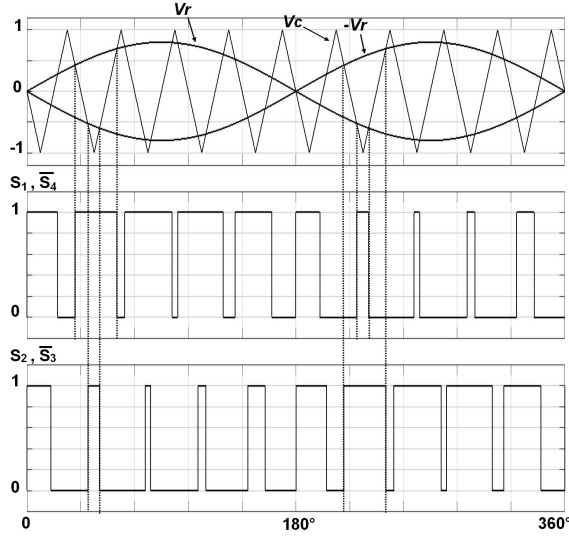


Fig. 6.  $V_c$ ,  $V_r$ ,  $-V_r$  signals and switches states

### C. The LC filter

Generally, The VSI must generate a sinusoidal waveform at the output of the inverter. But the voltage output is a combination of a fundamental component and harmonics. For this reason we need to design a suitable filter to eliminate harmonics [11]–[13]. In our case we used a modified LC filter. Paper [12] present a method that we add a series  $C_d$  and  $R_d$  in parallel with the shunt element of the filter to damp the resonance effects. The filter design is shown in figure 7 where we show also the element values that we used.

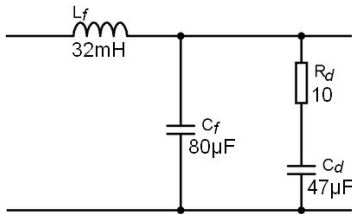


Fig. 7. Filter circuit.

### D. The load

The calibration performed has two aims. The first aim is to correct the current gain and the voltage gain at the input of the measurement circuit, to eliminate the errors due to the tolerances of the measurement components. The second aim is to compensate the phase shift between the voltage and the current which can be added by the measurement system to measure the exact active power [6]. In order to correct the gain of the amplifiers we have to measure known references (voltage and current). The reference voltage which is equal to  $120V_{RMS}$  will be stabilized by the control, and we have to size a load which will consume a reference current equal to  $5A_{RMS}$  and creates a phase shift equals  $60^\circ$ .

The load used is an inductive type. To calculate the values of the resistance and the inductance we use the following array:

$$\begin{cases} \sqrt{R_o^2 + (L_o\omega)^2} = V_o/I_o \\ L_o\omega/R_o = \tan 60 \end{cases} \quad (5)$$

After calculation, we obtain the following values:

$$R_o = 12\Omega, L_o = 66mH$$

### E. The controller

We used a digital control to control the inverter switches. This control is based on a microcontroller which must have the following features :

- Include an analog-to-digital converter (ADC) to convert the measured value of the input voltage to a digital value.
- Achieve a moderately high clock speed.
- Allows an interrupt on one of the timers to manipulate the time variable.

We can find these features in a PIC18F2550 microcontroller that contains a 10-bit ADC, allows an interrupt on the TIMER0 and the CPU clock can reach 48MHz. Before drawing the flowcharts of the program executed within the microcontroller, we will explain the method used to correct the signal.

1) *Method of correction:* From formula (4) we can write that (before the correction) the variation of the amplitude of the output signal is due to the variation of the input.

$$V'_{o1MAX}(t) = m_a V_{DC}(t) \quad (6)$$

To compensate the variations of the input we must adjust the value of  $m_a$  with each modification of  $V_{DC}(t)$ . Replacing  $m_a$  by its expression presented in formula (3) we get.

$$V'_{o1MAX}(t) = \frac{V_{rMAX}}{V_{cMAX}} V_{DC}(t) \quad (7)$$

We can notice that to adjust  $m_a$  we have two solutions: either adjust  $V_{cMAX}$  or adjust  $V_{rMAX}$ .

If we choose the adjustment of  $V_{rMAX}$ : We will adjust  $V_{rMAX}$  by taking into account the measured value of the input voltage at time t. Then we will calculate within the microcontroller the value of  $V_{rMAX}(t)$  at time t by:

$$V_{rMAX}(t) = V_{rINIT} \frac{V_{DC}}{V_{DC}(t)} \quad (8)$$

Where  $V_{r_{INIT}}$  is a value chosen at the time of initialization,  $V_{DC}$  is the reference value used to eliminate the variations and  $V_{DC}(t)$  is the DC voltage that contains variations. By replacing  $V_{r_{MAX}}$  of the formula (7) by the formula (8) found, we eliminate the variations and  $V'_{o1MAX}$  will only depend of constant values of  $V_{r_{INIT}}$ ,  $V_{c_{MAX}}$  and  $V_{DC}$ :

$$V'_{o1MAX} = \frac{V_{r_{MAX}}(t)}{V_{c_{MAX}}} V_{DC}(t) = \frac{V_{r_{INIT}}}{V_{c_{MAX}}} \frac{V_{DC}}{V_{DC}(t)} V_{DC}(t)$$

$$V'_{o1MAX} = \frac{V_{r_{INIT}}}{V_{c_{MAX}}} V_{DC} \quad (9)$$

The adjustment by acting on  $V_{c_{MAX}}$  follows the same procedure.

2) *Flowcharts of the program executed within the microcontroller:* Figure 8 contains two flowcharts. The flowchart (a) presents the sequences followed by the main function. The important task performed by this function is the real-time monitoring of the change in the value of the DC voltage, and the calculation of  $V_{r_{MAX}}$ . The flowchart (b) presents the sequences followed by the interrupt function. In this function we use a time variable (or step) that increments each interrupt on the TIMER0. We have programmed the different registers of the TIMER0 such that to have a step of 1/10 compared to the carrier signal period, i.e. a sampling frequency equals 10 times the frequency of the carrier signal. After incrementing the time variable we compare the value of Vr and the value of Vc at time t, and we control the switches S1 and S4; and then we compare the values of Vc and -Vr at the same time t, and we control the switches S2 and S3. It should be noted that since we use a high frequency clock, the code is executed quickly such that the switches are controlled at the same time.

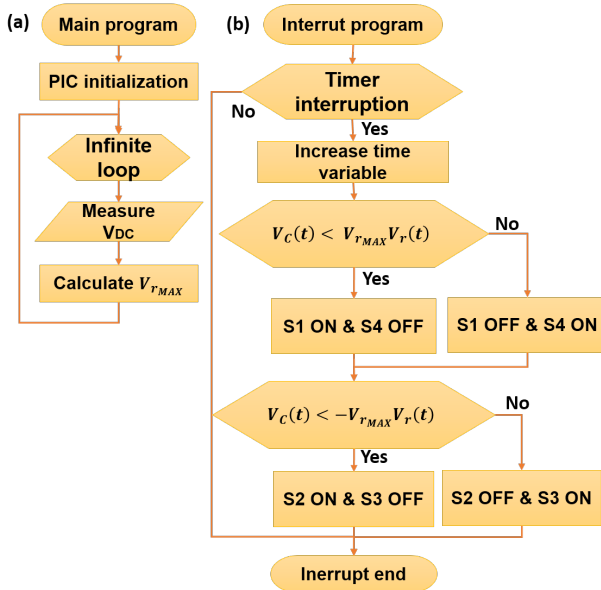


Fig. 8. Flowcharts of: (a) Main function and (b) Interrupt function

#### IV. SIMULATION AND RESULTS

To verify our design, we realized the circuit shown in figure 9. The realized circuit contains all the blocks mentioned before. To simplify the circuitry we used blocks called universal bridge for the rectifier and inverter blocks. As for the AC generator, we have built a variable generator which provides an alternating voltage increasing from the 249V value to the 358V value. We have modeled the function performed by the microcontroller by a block which has as input, an image of the voltage  $V_{DC}(t)$ , and outputs the control signal of the switches. In this block, the algorithm explained before is applied to correct the error. We present our results in three figures: The output voltage waveform in figure 12(b) and the output current waveform in the figure 12(a), the output voltage spectrum in the figure 10 and the output current spectrum in the figure 11. From these figures we deduce that:

- We obtained a very good waveform of the voltage  $V_O$  (figure 12 (b)). This is justified by the very low THD which equals 0.25% (figure 10).
- We obtained a very good waveform of the current  $I_O$  (figure 12 (a)). This is also justified by the very low THD which equals 0.04% (figure 11).
- We note in figure 12 (b) that even if the input voltage  $V_{AC}$  changes the amplitude, the output voltage remains stable. In addition the amplitude equals 169.6V (fundamental amplitude in figure 10) which corresponds to the RMS value 120V.
- From the figures 11 and 12 (b), the amplitude of the current equals 7.08A, which corresponds to the RMS value 5A.
- Finally, according to the figure 12, the delay between the voltage and the current equals  $\Delta t = 3.33ms$ , which corresponds to a phase shift equals  $60^\circ$ .

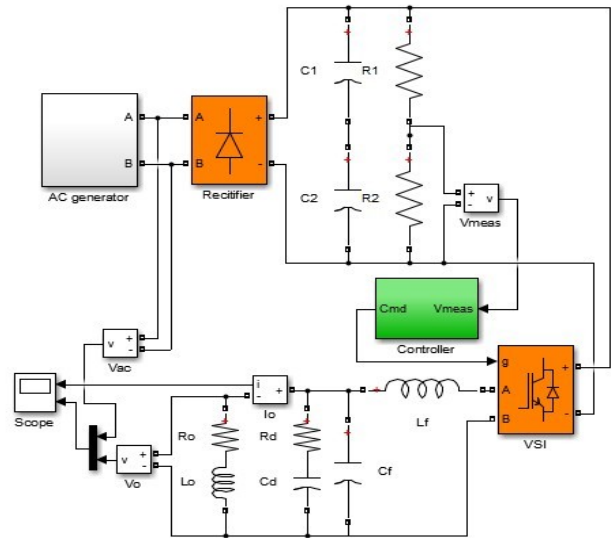


Fig. 9. Realized circuit on MATLAB for simulation

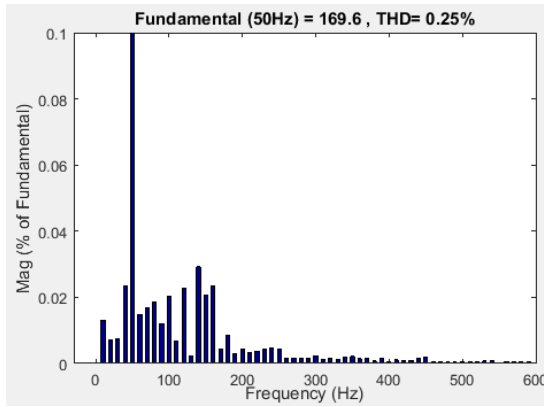


Fig. 10. AC output voltage spectrum

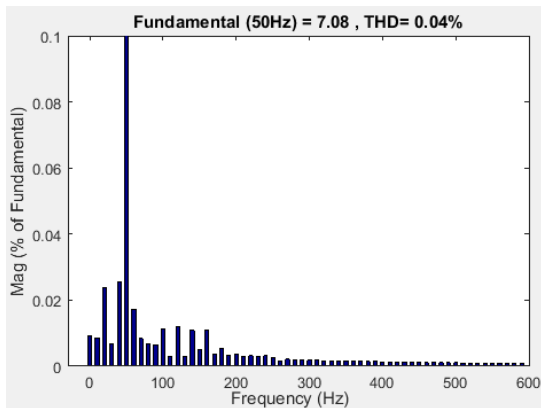


Fig. 11. AC output current spectrum

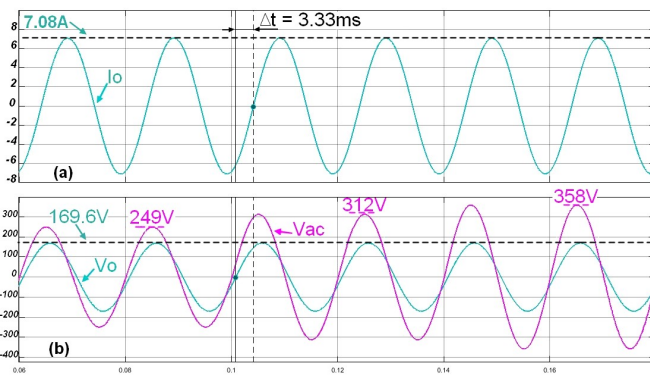


Fig. 12. Simulation results: (a) AC output current, (b) AC input voltage  $V_{AC}$  and AC output voltage  $V_o$

## V. CONCLUSION

Calibrating remotely the energy meters is a new approach introduced in smart meters. In order to be able to perform this operation remotely, we have integrated a calibration board which must provide a reference power during the calibration, since we can not directly use the voltage of the electrical grid which varies randomly and we can not know the exact value of the voltage at the calibration time. So, we opted to use an AC-AC converter powered by the electrical grid and provides

a fixed AC voltage. The structure of the converter is an indirect type AC-DC-AC.

To fix the AC output voltage of the converter, we used the feedforward technique to compensate variations in rectified DC voltage instead of measuring AC output voltage and correcting it. To control the switches of the DC-AC block taking into account the variation of input we used a digital control based on a microcontroller. Using the ADC module of the microcontroller, we measure the DC input voltage, we calculate the correction value and we generate the PWM signal based on the unipolar technique. The AC output voltage of the converter supplies a known load in order to determine the reference current. Moreover, this inductive load allows to create a phase shift between the voltage and the current. This phase shift is necessary to compensate that is added by the measurement system [6]. Our design of this converter is simulated on MATLAB. The results obtained validates our study, because we injected a signal that its amplitude vary while the amplitude of the AC output voltage of the converter remains stable. Moreover, the signal obtained is almost sinusoidal, this is justified by the low THD (0.25% for the voltage and 0.04% for the current).

## REFERENCES

- [1] M. Boutouba, A. E. Ougli, S. Miqoi, and B. Tidhaf, "Asymmetric Fuzzy Logic Controlled DC-DC Converter for Solar Energy system," *Journal of Renewable Energy and Sustainable Development*, vol. 2, no. 1, pp. 2356–8569, 2016.
- [2] M. Aamir and S. Mekhilef, "An Online Transformerless Uninterruptible Power Supply (UPS) System with a Smaller Battery Bank for Low-Power Applications," *IEEE Transactions on Power Electronics*, vol. 32, no. 1, pp. 233–247, 2017.
- [3] M. Aamir, K. A. Kalwar, and S. Mekhilef, "Review: Uninterruptible power supply (ups) system," *Renewable and Sustainable Energy Reviews*, vol. 58, pp. 1395 – 1410, 2016.
- [4] B. Perera, P. Ciuffo, and S. Perera, "Advanced point of common coupling voltage controllers for grid-connected solar photovoltaic (pv) systems," *Renewable Energy*, vol. 86, pp. 1037 – 1044, 2016.
- [5] A. Shboul, I. Safi, S. Alhawamdeh, and M. G. Batarseh, "Discussing single phase pwm voltage source inverters with different frequency modulation factors," in *2016 4th International Symposium on Environmental Friendly Energies and Applications (EFEA)*, Sept 2016, pp. 1–5.
- [6] Z. Jebrouni, H. Chadli, B. Tidhaf, A. Benlghazi, and A. Tahani, "Gain correction and phase compensation of a smart electrical energy meter," in *Engineering & MIS (ICEMIS), International Conference on*. IEEE, 2016, pp. 1–6.
- [7] Onee-be, *Compteurs numeriques d'energie electrique evolutif pour clients basse tension*, ONEE-BE, 2014.
- [8] A. Namboodiri and H. Wani, "Unipolar and Bipolar PWM Inverter," *IJIRSRT - International Journal for Innovative Research in Science & Technology*, vol. 1, no. 7, p. 7, 2014.
- [9] E. H. E. Aboadla, S. Khan, M. H. Habaebi, T. Gunawan, B. A. Hamidah, and M. Tohtayong, "Selective harmonics elimination technique in single phase unipolar h-bridge inverter," in *2016 IEEE Student Conference on Research and Development (SCORED)*, Dec 2016, pp. 1–4.
- [10] S. Maheshri and K. Prabodh, "Simulation of single phase spwm unipolar inverter," *International Journal of Innovative Research in Advanced Engineering (IJRAE)*, vol. 1, no. 3, 2014.
- [11] J. K. Steinke, "Use of an lc filter to achieve a motor-friendly performance of the pwm voltage source inverter," *IEEE Transactions on Energy Conversion*, vol. 14, no. 3, pp. 649–654, Sep 1999.
- [12] K. H. Ahmed, S. J. Finney, and B. W. Williams, "Passive filter design for three-phase inverter interfacing in distributed generation," in *2007 Compatibility in Power Electronics*, May 2007, pp. 1–9.
- [13] H.-S. Kim and S.-K. Sul, "A novel filter design for output lc filters of pwm inverters," *Journal of Power Electronics*, vol. 11, no. 1, pp. 74–81, 2011.